Evaluation of nitrogen balance in a direct-seeded-rice field experiment using Hydrus-1D

Yong Li [a,b,*], Jirka Šimůnek [c,*], Zhentin Zhang [b], Longfei Jing [b], Lixiao Ni [a,b]

[a] Ministry of Education Key Laboratory of Integrated Regulation and Resource Development on Shallow Lakes, Hohai University, Nanjing, 210098, China
[b] College of Environment, Hohai University, Nanjing, 210098, China
[c] Department of Environmental Sciences, University of California Riverside, Riverside, CA 92521, USA

ARTICLE INFO

ABSTRACT

Nitrogen (N) pollution is a global environmental problem that has greatly increased the risks of both the eutrophication of surface waters and contamination of ground waters. The majority of N pollution mainly comes from agricultural fields, in particular during rice growing seasons. In recent years, a gradual shift from the transplanting rice cultivation method to the direct seeding method has occurred, which results in different water and N losses from paddy fields and leads to distinct impacts on water environments. The N transport and transformations in an experimental direct-seeded-rice (DSR) field in the Taihu Lake Basin of east China were observed during two consecutive seasons, and simulated using Hydrus-1D model. The observed crop N uptake, ammonia volatilization (AV), N concentrations in soil, and N leaching were used to calibrate and validate the model parameters. The two most important inputs of N, i.e., fertilization and mineralization, were considered in the simulations with 220 and 145.5 kg ha^{-1} in 2008 and 220 and 147.8 kg ha^{-1} in 2009, respectively. Ammonia volatilization and nitrate denitrification were the two dominant pathways of N loss, accounting for about 16.0% and 38.8% of the total N input (TNI), respectively. Both nitrification and denitrification processes mainly occurred in the root zone. N leaching at 60 and 120 cm depths accounted for about 6.8% and 2.7% of TNI, respectively. The crop N uptake was 32.1% and 30.8% of TNI during the 2008 and 2009 seasons, respectively, and ammonium was the predominant form (74% of the total N uptake on average). Simulated N concentrations and fluxes in soil matched well with the corresponding observed data. Hydrus-1D could simulate the N transport and transformations in the DSR field, and could thus be a good tool for designing optimal fertilizer management practices in the future.

© 2014 Elsevier B.V. All rights reserved.

1. Introduction

Nitrogen (N) contamination of surface and ground waters has become a serious, global environmental problem (Chandna et al., 2011). The risk of groundwater contamination by N depends largely on the N input to agricultural fields in the form of inorganic fertilizers and on its effective use by agricultural crops (Becker et al., 2007). Paddy fields represent a special environment for the transport and transformations of N species due to their semi-artificial, alternate drying, and wetting conditions (Lüdemann et al., 2000; Ishii et al., 2011). Furthermore, diverse rice cultivation approaches may produce different types of N losses from paddy fields (Brar and Bhullar, 2013). The increasing cost and growing scarcity of labor, water, and fertilizers around the world has led to a conversion of the rice farming practice from traditional transplanting to direct seeding. There are three main types of direct-seeded-rice (DSR): dry, wet, and water direct-seeding, when rice seeds (with or without prior soaking) are directly sown onto dry, wet, and flooded soil, respectively, after land preparation (dry, wet, zero, reduced, or conventional tillage) (e.g., Farooq et al., 2011; Kumar and Ladha, 2011). Many researchers have previously reported that the DSR has different water management needs from TPR (Kumar and Ladha, 2011; Weerakoon et al., 2011). Additionally, some reports indicate that in DSR fields, most N is applied during the early-to-middle growth season (Naklang et al., 1996; Zhang and Wang, 2002; Yin et al., 2004; Brar and Bhullar, 2013), while in traditional TPR fields, about 40–60% of the total N fertilizer is applied as a basal fertilizer (Naklang et al., 1996; Hayashi et al., 2007; Chen et al., 2009).

Also, the distinct distribution of the root mass of DSR compared to TPR significantly influences the N fate and transport in paddy soils (Naklang et al., 1996). As a result, this shift of rice cultivation method, as well as tillage method, could result in different water and N losses from paddy fields, leading to different impacts on surface and ground water environments.

Due to the dynamic nature of paddy fields, N transport and transformation processes are complex and difficult to understand. Therefore, a fully calibrated, mathematical model that could describe these processes would be very useful. Although in recent years, a large number of researchers successfully evaluated the N balance in paddy fields using mathematical models, it is still a challenge to model N processes in paddy fields in their overall complexity. Some models focus mainly on N uptake and fate in floodwater (Jeon et al., 2004), while others pay more attention to the N transport in soils or describe the N cycle in soils without considering the N transport (Chowdary et al., 2004; Antonopoulos, 2010). In particular, the rhizosphere dynamics of N uptake is very complicated, since it may involve both passive and active uptake (Šimůnek and Hopmans, 2009), as well as other processes such as N mineralization, nitrification–denitrification, and rhizosphere acidity (Singh et al., 2011; Li and Wang, 2013; Najafi, 2013). Meanwhile, rice prefers ammonium (NH_4^+–N) to nitrate (NO_3^-–N) as a source of N (Ishii et al., 2011), and in the presence of both N species, rice seedlings take up NH_4^+–N faster than NO_3^-–N (Sasakawa and Yamamoto, 1978). However, in order to simplify the model and to limit the number of required parameters, many studies made the common assumption that the root uptake of NH_4^+–N and NO_3^-–N is strictly passive and other uptake mechanisms may be neglected (Hanson et al., 2006; Ravikumar et al., 2011; Ramos et al., 2012). This simplification may significantly affect the modeling of NH_4^+–N uptake and subsequent reactions and N distribution in the soil profile. Some studies also assumed homogeneous conditions in the soil profile and that the N transport and transformations could be simulated considering only one set of parameters for the entire soil profile while neglecting different conditions, and consequently different reaction parameters in different depths, due to changing aerobic and anaerobic conditions and soil layering (Chowdary et al., 2004).

Hydrus-1D (Šimůnek et al., 2008), a software package for simulating water flow and solute transport in soils, has been widely used to analyze flow and transport processes in TPR fields (Phogat et al., 2010) as well as in many other applications (Šimůnek et al., 2008; Sutanto et al., 2012). However, its use in DSR fields has been rather limited, especially with respect to simulating the N transport. In a companion paper, Li et al. (2014) successfully evaluated the use of Hydrus-1D to simulate water flow and water balance in DSR fields. They considered processes such as irrigation, precipitation, evaporation, surface runoff, and downward leaching and then quantified their contributions to the overall water balance. They also discussed the water use efficiency and crop yield. As a follow-up to this previous study, this paper's objective is to further extend their analysis to describe the transport and transformations of N in the same DSR field. This additional analysis will consider the processes such as the N transport, crop N uptake, ammonia

volatilization, nitrification–denitrification, and vertical N leaching. We will also discuss the N balance in the experimental DSR field.

2. Material and methods

2.1. Field experiments and measurements

2.1.1. Site description

The study site is located in the upstream region (31°56′N, 119°43′E) of the Taihu Lake Basin (TLB) in eastern China, which is classified as a flood plain because of frequent floodings of the Yangtze River. The climate is subtropical with periodical monsoon rains. Mean annual precipitation is 1181 mm (60% of which occurs from May through September) and the mean annual temperature is 15–17 °C. Field experiments were conducted in this area during two consecutive seasons (2008 and 2009). The soil layers of 0–60 cm and 60–120 cm were classified as silt loam and silt, respectively. Physical and hydraulic soil properties were described in detail in Li et al. (2014). Here, we will mainly list soil chemical properties (Table 1). The variety of rice used for DSR cultivation was *Wuxiangjing* 14 (lowland rice), a type of Japonica rice, which is predominantly cultivated in this region. The available N in the soil was about 220 kg ha^{-1}.

2.1.2. Experimental design

Field experiments were carried out in a 1350 m^2 (13.5 m × 100 m) paddy field, which was divided evenly into three plots (each about 13.5 m × 33.3 m), with each plot further subdivided into three sub-plots (each about 150 m^2) for replicating experiments. Five randomly selected sub-plots were used in this study. Each subplot had its own inlet (for irrigation) and outlet (for drainage) points. Averages of all observed data were used in comparisons with corresponding simulated values.

Details about the water management, as well as about evaporation, surface runoff, and drainage fluxes are described in Li et al. (2014). Total rainfall was 54.3 and 97.4 cm during 2008 and 2009 seasons, respectively, and 14 and 9 irrigations (each 5–6 cm) were applied, resulting in total irrigation water depths of 72 and 46 cm, respectively. The seed germination stage for dry DSR lasted for two weeks. To prevent long flooding and anaerobic conditions, and to control weeds, paddy fields need to be dried for about 5–10 days during each season, depending on the crop and soil conditions. The soil drying stage in the 2008 season was between August 7th and 12th (61–66 days after the basal fertilizer application, or DAB), while in the 2009 season it was between August 14th and 20th (65–71 DAB). The potential evapotranspiration, determined using the Penman–Monteith equation (Allen et al., 1998) and the crop coefficient, was divided into the potential evaporation and transpiration using observed values of *LAI* (Li et al., 2014).

The fertilization management was guided both by recommendations from the local Agricultural Technical Guidance Station and farmers' own experiences. The total quantity of N in each season was 220 kg N ha^{-1}, applied in five applications. The basal fertilizer (BF) was a compound fertilizer, consisting of about 15% of N,

Table 1
Selected physical and chemical properties of the soil in the experimental DSR field in the Taihu Lake Basin.

Depth (cm)	Texture	Bulk density (g cm^{-3})	Organic matter (g kg^{-1})	CEC (cmol kg^{-1})	pH (H$_2$O)	Total Nitrogen (g kg^{-1})	NH_4^+–N (mg kg^{-1})	NO_3^-–N (mg kg^{-1})
0–20	Silt loam	1.42	5.1	14.6	6.65	1.54	4.6	6.2
20–40		1.56	5.4	13.7	6.85	0.62	3.1	5.8
40–60		1.51	3.7	10.7	6.85	0.34	2.4	4.7
60–80	Silt	1.43	3.5	11.3	6.80	0.31	1.2	5.1
80–100		1.43	3.3	9.4	6.80	0.24	1.3	4.3
100–120		1.43	3.3	9.1	6.85	0.22	1.4	3.4

Table 2
Agricultural activities in the experimental DSR field during the 2008 and 2009 seasons.

2008	2009	Agricultural activities
Jun. 8	Jun. 11	Basal fertilizer (33 kg N ha^{-1}, 33 kg P ha^{-1}, 33 kg K ha^{-1}) plowed in by machines within 5 cm top soil; Sowing by hand (75.0 kg of seeds ha^{-1}).
Jun. 8–21	Jun. 11–24	Germination stage
Jun. 27	Jun. 25	Seedling fertilizer (44 kg N ha^{-1})
Jul. 13	Jul. 12	Tillering fertilizer (55 kg N ha^{-1})
Jul. 30	Jul. 31	Jointing fertilizer (44 kg N ha^{-1})
Aug. 7–12	Aug. 13–19	Soil drying stage
Aug. 20	Aug. 22	Panicle fertilizer (44 kg N ha^{-1}, 12 kg P ha^{-1}, 12 kg K ha^{-1})
Nov. 1	Nov. 5	Harvest

phosphorus, and potassium. During four additional applications, fertilizer was top-dressed (TF) in the form of urea (the content of N was about 46%) at the following rates: 44 (TF$_1$), 55 (TF$_2$), 44 (TF$_3$), and 44 (TF$_4$) kg N ha^{-1}. During land preparation, the BF was applied without floodwater and plowed within 5 cm of the top soil by agricultural machinery, while each TF was evenly broadcasted by hand in floodwater. Detailed agricultural activities are listed in Table 2.

2.1.3. Measurements and analysis

Samples of surface runoff water were collected hourly from the outlet points when they were draining. The cumulative N loss due to surface runoff was calculated by multiplying water flux with corresponding NH$_4^+$–N and NO$_3^-$–N concentrations. Soil solutions were collected once a week throughout the growing season using porous ceramic cups (PCCs, 60 mm long). The PCCs were installed at 20, 40, 60, 80, and 100 cm depths before rice seeding. Each time before sampling, the residual solution in each cup was cleansed using an injector. The PCCs were then evacuated to about 80 kPa by a vacuum pump with a tensiometer. About 1.5 h later, the solutions in the PCCs could be extracted for further analysis. The cumulative N leaching at the 60 cm depth was determined by multiplying the N concentrations with corresponding water fluxes (Li et al., 2014) and integrating over the entire season. All water samples and soil solutions were filtered through a 0.2-μm membrane filter. The NH$_4^+$–N and NO$_3^-$–N concentrations were measured using standard colorimetric methods and flow injection analysis.

Ammonia (NH$_3$) volatilization (AV) was measured using the H$_2$SO$_4$ trap method (Sarkar et al., 1991; Kyaw et al., 2005). The AV rate was observed daily after the fertilizer application and then twice weekly thereafter. Samples of three replications were taken for each morning or afternoon measurement. The total ammonia emission during a season was calculated by integrating linearly interpolated gas emissions on sampling days.

Rice growth was observed on 15, 30, 45, 60, 75, 90, 105, 120 DAB, and on the harvest day. The plants were separated into grain, straw, and roots, and then oven dried at 70 °C. The dried samples were weighed, ground, and prepared for chemical analysis. Total N (TN) content in the plant samples was determined by automatic combustion in tin (Sn) capsules and analyzed using a stable isotope mass spectrometer. Cumulative total N uptake was determined as the product of the TN content of the rice tissue and the dry weight (Kyaw et al., 2005).

2.2. Hydrus-1D model

2.2.1. Model description

Hydrus-1D allows for simultaneously considering the fate and transport of multiple solutes that are subject to first-order degradation reactions. The first-order decay chain of urea can be described as follows (Hanson et al., 2006):
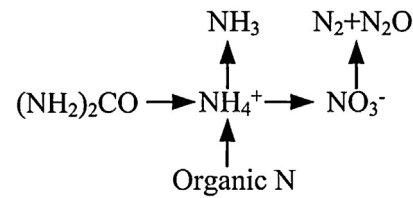
The following N transformation processes were considered here: (1) hydrolysis of urea to NH$_4^+$–N; (2) mineralization of organic N to NH$_4^+$–N; (3) ammonia volatilization; (4) nitrification of NH$_4^+$–N to NO$_3^-$–N; (54) denitrification of NO$_3^-$N; (6) adsorption of NH$_4^+$–N; and (7) rice root uptake of NH$_4^+$–N and NO$_3^-$–N. Hydrolysis, nitrification, and denitrification are all considered as first-order reactions (Hanson et al., 2006), while mineralization is considered to be a zero-order process.

The partial differential equations governing one-dimensional transport of N involved in sequential first-order decay chain reactions during transient water flow in a variably-saturated rigid porous medium are taken as (Šimůnek et al., 2008):

$$\frac{\partial \theta C_1}{\partial t} = \frac{\partial}{\partial z}\left(\theta D_1^w \frac{\partial C_1}{\partial z}\right) - \frac{\partial q C_1}{\partial z} - \mu'_{w,1}\theta C_1 \tag{1}$$

$$\frac{\partial \theta C_2}{\partial t} + \frac{\partial \rho S_2}{\partial t} + \frac{\partial a_v g_2}{\partial t} = \frac{\partial}{\partial z}\left(\theta D_2^w \frac{\partial C_2}{\partial z}\right) + \frac{\partial}{\partial z}\left(a_v D_2^g \frac{\partial g_2}{\partial z}\right) - \frac{\partial q C_2}{\partial z}$$
$$- \mu'_{w,2}\theta C_2 + \mu'_{w,1}\theta C_1 + \gamma_{s,2}\rho - r_{a,2} \tag{2}$$

$$\frac{\partial \theta C_3}{\partial t} = \frac{\partial}{\partial z}\left(\theta D_3^w \frac{\partial C_3}{\partial z}\right) - \frac{\partial q C_3}{\partial z} - \mu_{w,3}\theta C_3 + \mu'_{w,2}\theta C_2 - r_{a,3} \tag{3}$$

where, C is the solute concentration in the liquid phase (mg L^{-1}); S is the solute concentration in the solid phase (mg g^{-1}); g is the solute concentration in the gas phase (mg L^{-1}); θ is the volumetric water content (cm^3 cm^{-3}); ρ is the dry bulk density (g cm^{-3}); q is the volumetric flux density (cm day^{-1}), μ_w is the first-order rate constant for solute in the liquid phase (day^{-1}); μ'_w is a similar first-order rate constant, providing connections between individual chain species; γ_s is a zero-order rate constant in the solid phase (day^{-1}); r_a is the root nutrient uptake (mg L^{-1} day^{-1}); D_w is the dispersion coefficient (cm^2 day^{-1}) for the liquid phase, and D^g is the diffusion coefficient (cm^2 day^{-1}) for the gas phase. The subscripts 1, 2, and 3 represent (NH$_2$)$_2$CO, NH$_4^+$–N, and NO$_3^-$–N, respectively.

Adsorption/desorption of NH$_4^+$ is considered to be an instantaneous reaction between the soil solution and the exchange sites of the soil matrix (Nakasone et al., 2004). The adsorption isotherm relating S_2 and C_2 is described using a linear equation of the form:

$$S_2 = K_{d,2} C_2 \tag{4}$$

where, $K_{d,2}$ is the distribution coefficient for NH$_4^+$ (L mg^{-1}).

2.2.2. Input parameters

The input parameters for the solute transport part of Hydrus-1D are required to characterize the three main sets of processes: solute transport, solute reactions/transformations, and root solute uptake. The solute transport parameters were considered using the following values: the molecular diffusion coefficients in free water (D^w) for NH$_4^+$–N and NO$_3^-$–N were 1.52 and 1.64 cm^2 day^{-1}, respectively, the molecular diffusion coefficient in air (D^a) for NH$_3$ was 18057.6 cm^2 day^{-1}, the longitudinal dispersivity (12 cm) was considered equal to one-tenth of the profile depth (Phogat et al., 2012), and the Henry's law constant (K_H, at 25 °C) for NH$_4^+$–N was 2.95×10^{-4} (Renard et al., 2004). The distribution coefficient (K_d) for NH$_4^+$ and for different soil layers is listed in Table 3, based on values for this region reported by Chen and Chiang (1963).

The N reaction parameters were initially taken from the literature (Chowdary et al., 2004) and then corrected for individual

Table 3
Reaction parameters for N transformations obtained by model calibration (K_{mi} is the comprehensive production rate of NH_4^+ representing mineralization/immobilization; K_d is the distribution coefficient for NH_4^+; K_n is the nitrification rate; K_{dn} is the denitrification rate; and K_h is the urea hydrolysis rate).

Soil depth (cm)	K_m (day^{-1})	K_d (L mg^{-1})	K_n (day^{-1})	K_{dn} (day^{-1})	K_h (day^{-1})
0 − 20	0.0045	1.8	0.25	0.05	0.74
20 − 40	0.0045	1.5	0.22	0.06	
40 − 60	−	1.2	0.14	0.04	
60 − 80	−	1.0	0.04	0.02	
80 − 100	−	1.0	0.02	0.01	
100 − 120	−	1.0	0.02	0.01	

soil layers to fit observed data (Table 3). The urea hydrolysis rate K_h was assumed equal to 0.74 day^{-1} in the top soil layer (0–20 cm). Mineralization (organic N→inorganic NH_4^+–N) and immobilization (inorganic NH_4^+–N→organic N) are two important N transformation processes that occur simultaneously in flooded soils (Chowdary et al., 2004). We assumed here that these two transformations occurred only in the root zone (Rice and Smith, 1984) (0–40 cm), and that they can be represented by a single comprehensive production rate for NH_4^+–N K_{mi} of 0.0045 day^{-1} (Yan et al., 2006; Antonopoulos, 2010; Roberts et al., 2011). The nitrification and denitrification rates were initially assumed to be the same in all soil layers (namely $K_n = 0.2$ day^{-1} and $K_{dn} = 0.04$ day^{-1}) and then adjusted for each layer according to observed data. While some of these processes are temperature and water content dependent, it is a common practice to neglect these dependences (Chowdary et al., 2004; Hanson et al., 2006).

The average daily N uptake rates were calculated using linear interpolation for each time interval between two observed N crop data (in the 2008 season). Unlimited passive uptake of NO_3^-–N was allowed in the root solute uptake model (Šimůnek and Hopmans, 2009) by specifying the maximum allowed uptake concentration exceeding NO_3^-–N concentrations that were registered in the root zone. By considering active uptake in addition to passive uptake for NH_4^+–N, contrary to considering only passive uptake for NO_3^-–N, we could ensure that NH_4^+–N uptake accounts for approximately 75% of the total N uptake (Kirk and Kronzucker, 2005; Li et al., 2006). The Michaelis–Menten constant for the active uptake of NH_4^+ was assumed equal to 0.31 mg L^{-1} (Wang et al., 1994; Duan et al., 2007).

2.2.3. Initial and boundary conditions

The initial conditions for water flow were defined using the observed pressure heads. The initial ammonium and nitrate contents in the soil were specified in terms of N concentrations in soil water according to observed data. The initial concentration of urea was calculated from the initial application of the basal fertilizer and the initial water content, while assuming that urea was mixed within the surface 5-cm soil layer.

An atmospheric boundary condition with surface runoff (during the first two weeks and during the drying stage) or with a surface layer (during the rest of the season), which needs to be reached before surface runoff is initiated, was specified at the soil surface for water flow. The constant pressure head boundary condition was considered at the bottom boundary, reflecting the position of the groundwater table (Li et al., 2014). Root water uptake was calculated using the potential evapotranspiration rate, calculated using the Penman–Monteith equation (Allen et al., 1998), a given rooting depth and density, and the Feddes' stress response function (Feddes et al., 1978). The top boundary for solute transport was set as a 'volatile' boundary condition (Jury et al., 1983) with a stagnant boundary layer of 2.5 cm (calibrated using observed AV data from the 2008 season). This boundary condition assumes that there is a stagnant boundary layer (air) at the top of the soil profile and that solute movement through this layer is by solute diffusion in air. A third-type boundary condition was used at both the top and bottom boundaries. The top-dressed fertilizer application was

represented in the model by converting the amount of applied urea into the boundary concentration using the known value of the surface water layer (from the previous simulation of water flow) at the time of fertilizer application. The concentration fluxes of N for all four urea applications were calculated assuming a molar mass and a number of atoms for each molecule.

2.3. Model evaluation

Simulated values of inorganic N (NH_4^+–N and NO_3^-–N) concentrations in the soil, cumulative N leaching fluxes at 60 cm depth, and the total N uptake by rice were compared with the observed data. The correspondence between simulated and observed data was evaluated using the coefficient of correlation (r^2) at $p = 0.05$ and the root mean square error (RMSE). The RMSE was calculated as

$$\text{RMSE} = \sqrt{\frac{1}{n}\sum_{1}^{n}(S_i - M_i)^2} \qquad (5)$$

where, S_i and M_i are simulated and observed values, respectively, and n is the number of values compared. The optimum values of r^2 and RMSE are 1 and 0, respectively.

3. Results and discussion

3.1. Model calibration and validation

The calibration and validation of complex numerical models are often complicated due to many parameters that need to be simultaneously determined. Since all parameters related to water flow have been previously reported (Li et al., 2014), only the parameters related to N transformations were calibrated and are discussed here. The observed data during the 2008 season were used for model calibration. First, the input of mineral N consists of two pathways, i.e., applications of mineral fertilizer and the mineralization of organic N. The mineralization rate was thus determined based on fertilizer applications and soil organic N (Chowdary et al., 2004; Li et al., 2011). Second, observed AV fluxes and their cumulative quantity were used to calibrate the thickness of the stagnant boundary layer for gas diffusion (2.5 cm). Third, the daily NH_4^+–N active uptake rates were calibrated based on observed crop N data. Finally, observed concentrations of NH_4^+–N and NO_3^-–N at 20, 40, 60, and 80 cm depths and a leaching flux at the 60 cm depth were used to determine the nitrification and denitrification rates for each soil layer. After successful model calibration, observed data from the 2009 season were used for model validation. The r^2 and RMSE values were calculated to evaluate the effectiveness of the model input (calibrated) parameters.

Fig. 1(a) and (b) shows that simulated N concentrations at different depths during the 2008 season agreed with observed data well, with $r^2 = 0.99$ and RMSE = 0.13 mg L^{-1} ($n = 87$) for NH_4^+–N, and $r^2 = 0.98$ and RMSE = 0.40 mg L^{-1} ($n = 88$) for NO_3^-–N. Similar results (Fig. 1(c) and (d)) were also obtained for the 2009 validation
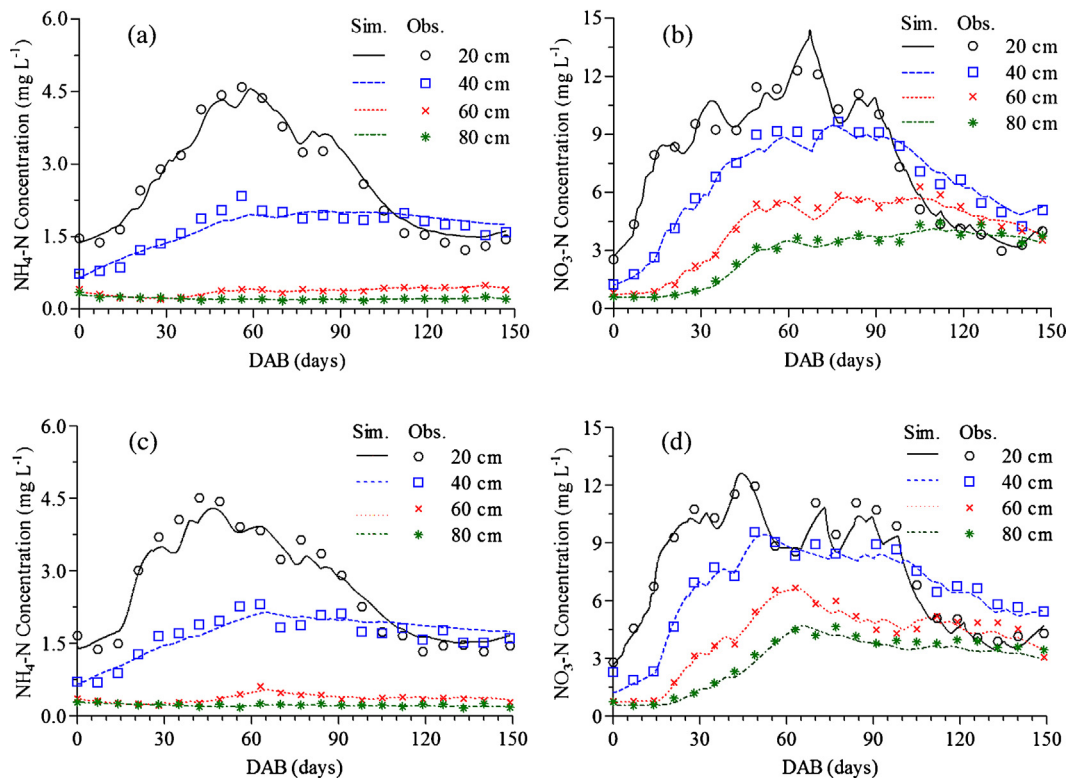
Fig. 1. Comparison of simulated (Sim) and observed (Obs) NH_4^+–N (a, c) and NO_3^-–N (b, d) concentrations at 20, 40, 60, and 80 cm depths during the 2008 (a, b) and 2009 (c, d) seasons.

season, with $r^2 = 0.98$ and RMSE = 0.17 mg L^{-1} ($n = 88$) for NH_4^+–N, and $r^2 = 0.98$ and RMSE = 0.41 mg L^{-1} ($n = 87$) for NO_3^-–N. The calibration and validation results for N plant uptake and the AV and N leaching fluxes will be discussed in different sections below. Overall, Fig. 1 shows that the final set of parameters adopted for Hydrus-1D simulations (listed in Table 3) were reasonable and effective for simulating the N transport and transformations in the DSR experimental field.

3.2. Ammonia volatilization

The comparison of simulated and observed ammonia volatilization (AV) fluxes from the experimental DSR field during the two seasons is shown in Fig. 2. Overall, AV increased and then rapidly dropped after each fertilizer application. After 2 DAB, the AV fluxes reached peak values of about 1.7 and 2.0 kg ha^{-1} day^{-1} during the 2008 and 2009 seasons, respectively, and quickly dropped within 7–10 days. This was due to high concentrations of NH_4^+–N in surface soil with low water contents after BF was applied. Both simulated and observed data then showed lower peak values of the AV rate in response to subsequent fertilizer applications (TFs). In particular, AV after the third topdressing of fertilizer (TF_3) during the 2009 season was low, partly due to a low concentration of NH_4^+ in floodwater (Fig. 3) and partly due to large N loss (4.8 kg ha^{-1}) by surface runoff (8.1 cm). On the other hand, the rapid decline in AV after TF_2 may be attributed to a higher absorption of fertilizer N by the well-developed root system in the top soil layer at this stage of crop growth (Schnier et al., 1990). This may also explain the low NH_4^+–N concentrations in floodwater after the TF_2 application (Fig. 3).

Simulated peak values of AV were slightly lower than the corresponding observed data, but the fluxes between peaks, as well as the overall trend, matched very well with observed data. Meanwhile, observed data show that after each fertilizer application,

AV proceeded faster than simulated. The simulated cumulative AV fluxes were 63.4 and 58.6 kg ha^{-1} during the 2008 and 2009 seasons, respectively, with averages of 0.43 and 0.39 kg ha^{-1} day^{-1}; the observed data were 56.2 and 52.6 kg ha^{-1}, with averages of 0.38 and 0.35 kg ha^{-1} day^{-1}, respectively. The difference between the two seasons was mainly ascribed to the different AV fluxes after the applications of TF_2 and TF_3 that resulted from different NH_4^+–N concentrations within variable depths of floodwater.

When compared with other studies in this region, our simulated and observed AV values fell within reported ranges. Cao et al. (2013) reported that the total NH_3 losses from the TPR fields were 51.6 and 49.2 kg N ha^{-1} during the 2009 and 2010 seasons, which accounted for 17.2% and 16.4% of the total N fertilizer, respectively. Zhu et al. (2004) and Li et al. (2008) reported that the N losses through AV in the TPR fields were about 18.6–38.7% and 9.6–33.7% of the total N fertilizer, respectively. Zhang et al. (2011a,b) also reported that the mean AV fluxes ranged from 0.29 to 0.53 kg ha^{-1} day^{-1} in the DSR fields of central China. Overall, the Hydrus-1D model produced a good correspondence between observed and simulated AV fluxes during the 2008 ($n = 73$, $r^2 = 0.73$, RMSE = 0.26 kg ha^{-1} day^{-1}) and 2009 ($n = 62$, $r^2 = 0.78$, RMSE = 0.24 kg ha^{-1} day^{-1}) seasons.

3.3. Nitrogen concentrations in floodwater and its loss due to surface runoff

Fig. 3 shows the observed NH_4^+–N and NO_3^-–N concentrations in floodwater during both seasons and compares them with simulated concentrations in the soil surface observation point, which represents the model floodwater. After the fertilizer was applied, the concentrations of NH_4^+–N and NO_3^-–N increased and then quickly declined. Meanwhile, the NO_3^-–N concentrations lagged behind those of NH_4^+–N. During the 2008 season, the N concentrations increased much less after the TF_2 application than after other TFs, because subsequent surface runoff
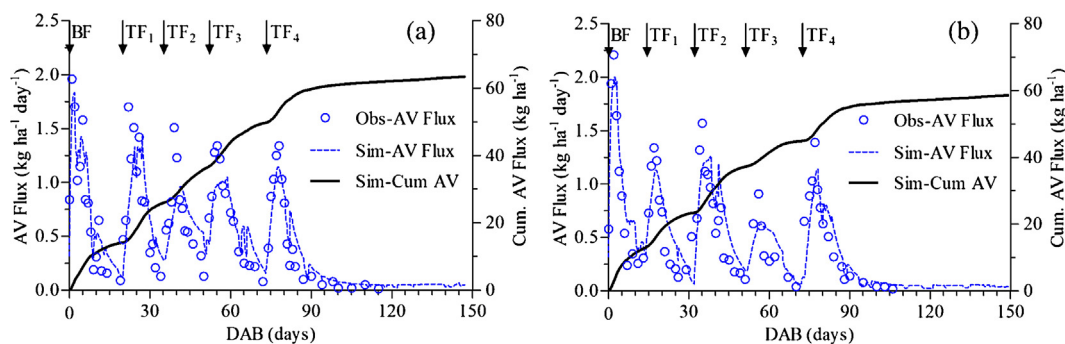
Fig. 2. Comparison of simulated and observed ammonia volatilization (AV) fluxes and simulated cumulative AV fluxes during the 2008 (a) and 2009 (b) seasons. The arrows at the top indicate fertilizer applications.

removed large amounts of N (5.0 kg ha^{-1}). During the 2009 season, the low concentrations after the TF$_3$ application were ascribed to the relatively high depth of floodwater. Observed NH$_4^+$–N and NO$_3^-$–N during the 2008 season were within the range of 0.13–16.30 mg L^{-1} (average of 3.42 mg L^{-1}) and 0.79–13.11 mg L^{-1} (average of 5.10 mg L^{-1}), respectively; during the 2009 season, they ranged from 0.11 to 12.18 mg L^{-1} (average of 3.25 mg L^{-1}) and from 0.64 to 18.32 mg L^{-1} (average of 4.80 mg L^{-1}), respectively. Simulated values matched the observed data with a relatively low $r^2 = 0.18$ and high RMSE = 3.5 mg L^{-1} ($n = 117$) for NH$_4^+$–N and $r^2 = 0.49$ and RMSE = 2.42 mg L^{-1} ($n = 113$) for NO$_3^-$–N during the two seasons. However, the overall trend of simulated N concentrations matched the observed data well.

In China's TLB, the N loss due to surface runoff usually occurs in the early season because of intensive, typhoon-like rainfall. Both seasons (2008 and 2009) had a very different distribution of precipitation, which resulted in significantly different surface runoff and associated N loss. The simulated surface runoff amounted to 24.4 cm during the 2009 season, which was approximately four times more than in the 2008 season (5.8 cm) (Li et al., 2014). The simulated N losses due to surface runoff in the two seasons were 10.3 and 17.0 kg ha^{-1}, respectively. Qiao et al. (2012) reported that N losses due to surface runoff from TPR fields in this region were 12.0 and 47.0 kg ha^{-1} (for the total N fertilizer application of 216 kg ha^{-1}) during the 2008 and 2009 seasons, respectively. Zhao et al. (2012) reported that N runoff from paddy soil (TPR) varied from 2.65 to 21.8 kg N ha^{-1} during three seasons (2007–2009) in this region.

The average concentrations of NH$_4^+$–N + NO$_3^-$–N in surface runoff in 2008 and 2009 were 17.7 and 7.0 mg L^{-1}, respectively. The major N loss (accounting for about 71% of the total runoff loss) in 2008 occurred during the second surface runoff event just one day after the TF$_2$ application when NH$_4^+$–N and NO$_3^-$–N

concentrations were still relatively high. While NH$_4^+$–N and NO$_3^-$–N concentrations in surface runoff were relatively low during the 2009 season, a large amount of surface runoff still removed high levels of N (19.2 kg ha^{-1}).

3.4. Crop nitrogen uptake

While NH$_4^+$–N uptake by rice was simulated in Hydrus-1D as both passive and active uptake, NO$_3^-$–N was only simulated as a passive uptake (Šimůnek and Hopmans, 2009). As shown in Fig. 4, the uptake process proceeded relatively slowly after sowing, gradually increased during seedling stages, and reached about 12.8 (in 2008 season) and 12.6 kg ha^{-1} (in 2009) on 30 DAB. After the germination stage and through TFs applications, the crop grew quickly and absorbed large quantities of N. At later stages, the N uptake remained relatively stable, ultimately reaching 114.8 (2008) and 112.1 kg ha^{-1} (2009). The average N uptake fluxes were approximately 0.78 and 0.75 kg ha^{-1} day^{-1} throughout both seasons, respectively. Similar results were reported for DSR fields in the Philippines (110–139 kg ha^{-1} (Mnguu, 2010); 105–118 kg ha^{-1} (Schnier et al., 1990)). Since the root mass of DSR is distributed shallower and more evenly in the soil (Naklang et al., 1996; Yadav et al., 2007) compared to TPR, most uptake of water and nutrients occurred in the shallower soil layer.

In the two seasons, most N was absorbed in the NH$_4^+$–N form, which accounted for about 74% of total N uptake on average. Zhang et al. (2011a,b) reported, based on hydroponic experimental studies, that during the seedling stage, about 2/3 of rice N uptake was in the NH$_4^+$–N form. Kirk and Kronzucker (2005) reported that lowland rice absorbs NH$_4^+$–N (60–85%) as a major source of N. Li et al. (2006) also reported that during a 96-h hydroponic experiment with the NH$_4$NO$_3$ solution, the uptake of NH$_4^+$–N by rice roots accounted for approximately 63% of total N uptake.
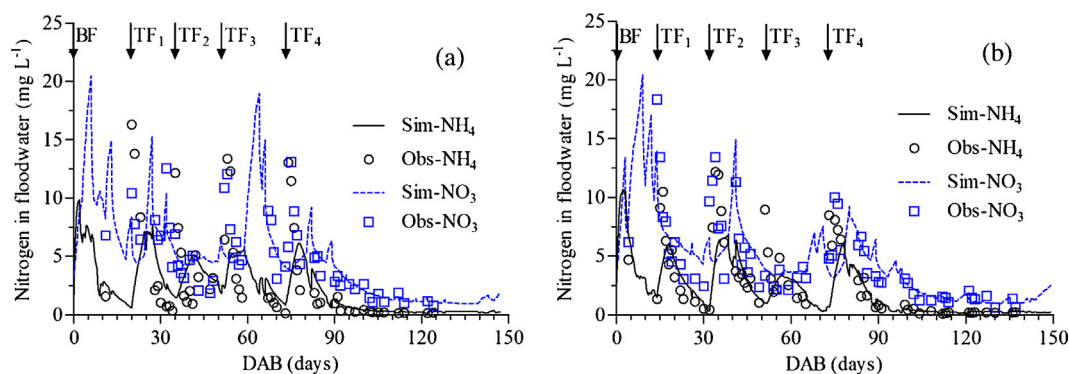
Fig. 3. Comparison of simulated and observed nitrogen (NH$_4^+$–N and NO$_3^-$–N) concentrations in floodwater during the 2008 (a) and 2009 (b) seasons.
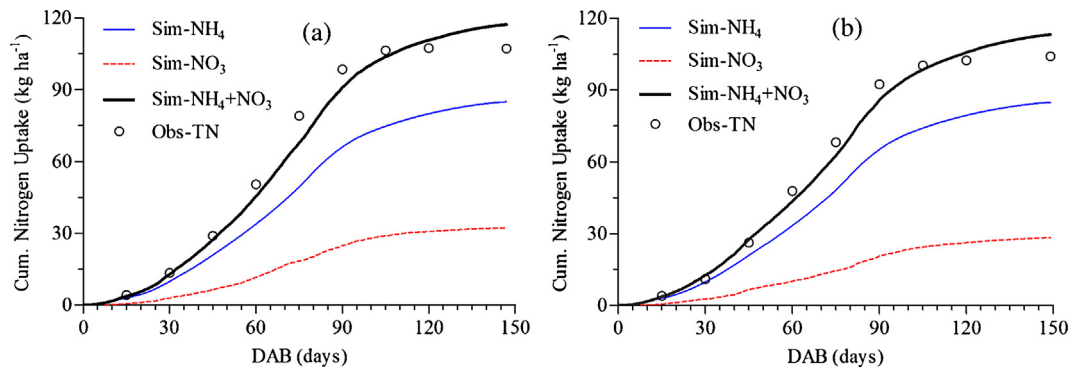
Fig. 4. Simulated cumulative nitrogen (NH_4^+–N, NO_3^-–N, and total) uptake and observed total nitrogen uptake during the 2008 (a) and 2009 (b) seasons.

Overall, simulated values of N uptake matched the observed data well (2008 season: $n = 9$, $r^2 = 0.98$, RMSE = 6.1 kg ha^{-1}; 2009 season: $n = 9$, $r^2 = 0.98$, $RMSE = 3.3$ kg ha^{-1}), with only slight overestimation during the late stage. This implies that the N uptake parameters in Hydrus-1D were reasonable and could be adapted to simulate the N uptake process of DSR.

3.5. Nitrogen leaching

Fig. 5 shows the simulated cumulative N fluxes at 0, 20, 40, and 60 cm depths during the two seasons. Although rainfall, runoff, and irrigation were quite different between the two seasons (Li et al., 2014), vertical fluxes showed similar trends. Virtually the entire vertical flux of NH_4^+–N at the soil surface occurred before 90 DAB, when surface fertilizer applications took place. On the other hand, cumulative vertical fluxes of NH_4^+–N at 20, 40, and 60 cm depths continued to slowly increase later in the season. This was mainly because there was an additional important source of NH_4^+–N in the top two soil layers: the mineralization of organic N. About 22.2 and 20.9 kg ha^{-1} of NH_4^+–N infiltrated into the soil profile during the 2008 and 2009 seasons, respectively. The total vertical flux of NH_4^+–N at 40 cm fell to 9.4 (2008) and 9.1 kg ha^{-1} (2009), due to various processes that removed NH_4^+–N from the top soil layers, such as AV, root N uptake, and nitrification in the root zone (Hou et al., 2007). Contrary to NH_4^+–N, NO_3^-–N fluxes at the soil surface were slightly lower than those at 20 cm. This was mainly due to processes that increased NO_3^-–N concentrations in the root zone, which was mainly nitrification of NH_4^+–N. While NO_3^-–N was absorbed by rice roots and denitrified in the root zone, large quantities of NO_3^-–N remained in the soil and were quickly transported downward along with leaching water. The average total flux at 40 cm was approximately 37.5 kg ha^{-1}, which was almost similar to that at the soil surface (45.0 kg ha^{-1}).

Observed concentrations of NH_4^+–N (0.20–0.62 mg L^{-1}) and NO_3^-–N (0.76–6.67 mg L^{-1}) at 60 cm showed that NO_3^-–N was the dominant N form (on average 92.3% of the NH_4^+–N + NO_3^-–N) in percolating water during the two seasons. Similar results were reported by Zhang et al. (2011a,b) from DSR fields in Central China. Kyaw et al. (2005) also found that NH_4^+–N accounted for only about 3–5% of total N leaching at 35 cm in a TPR field. The simulated cumulative N fluxes at 60 cm agreed well with the observed data during the two seasons with $r^2 = 0.98$ and RMSE = 0.12 mg L^{-1} for NH_4^+–N ($n = 20$), and $r^2 = 0.97$ and RMSE = 1.38 mg L^{-1} for NO_3^-–N ($n = 20$).

N leaching is closely correlated with vertical water flow. As shown in Fig. 6, the N leaching distributions at the bottom of the soil profile (120 cm) are similar to the corresponding water flux distributions (Li et al., 2014). During the 2008 season, the N leaching mainly occurred in middle-to-late season, especially after the soil drying stage, with frequent irrigation events. During the 2009 season, relatively high and continuous leaching occurred during 40–65 DAB before the soil-drying stage, with subsequent intermittent N leaching events corresponding to irrigation events. The leaching fluxes of NH_4^+–N during the two seasons were relatively stable and remained within 0–0.017 kg ha^{-1} day^{-1} (average of 0.007 kg ha^{-1} day^{-1}). Reduced oxygen in the rhizosphere for long periods of time prevented nitrification of NH_4^+–N and leaching of this form of N (Kirk et al., 1994). Note that NH_4^+–N, contrary to NO_3^-–N, is adsorbed to soil and thus its leaching is significantly retarded. Contrary to NH_4^+–N fluxes, NO_3^-–N fluxes widely and frequently varied along with the water flux, and fell in a relatively wide range of 0.002–0.180 kg ha^{-1} day^{-1} (average of 0.063 kg ha^{-1} day^{-1}) in the 2008 season and 0.001–0.168 kg ha^{-1} day^{-1} (average of 0.057 kg ha^{-1} day^{-1}) in the 2009 season.

The simulated cumulative N leaching at 120 cm was 10.3 and 9.5 kg ha^{-1} during the 2008 and 2009 seasons, respectively, with
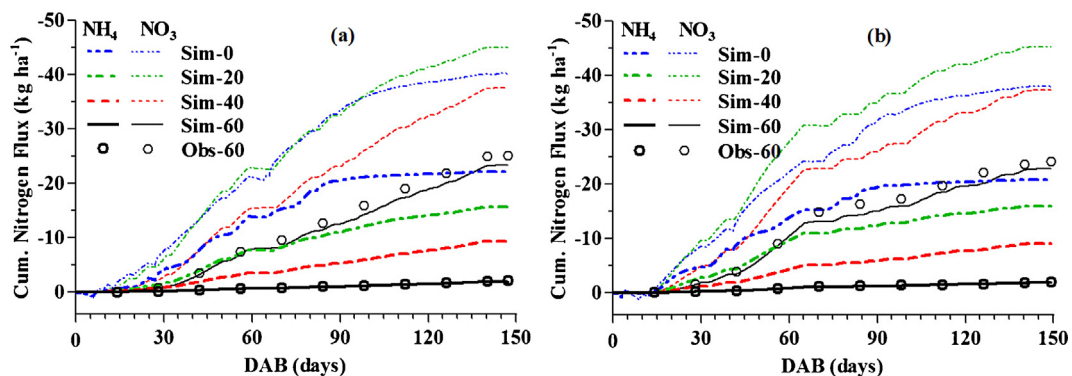

Fig. 5. Simulated cumulative nitrogen fluxes at 0, 20, 40, and 60 cm depths below the soil surface and observed cumulative nitrogen fluxes at the 60 cm depth during the 2008 (a) and 2009 (b) seasons.
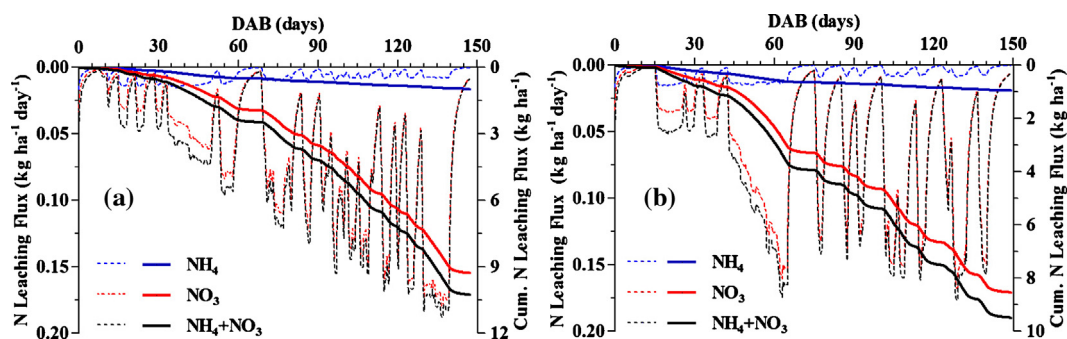
Fig. 6. Simulated nitrogen leaching fluxes (thin dotted lines) and cumulative fluxes (thick solid lines) at the bottom of the soil profile (120 cm) during the 2008 (a) and 2009 (b) seasons.

NO_3^-–N accounting for most of it (about 90%). Most NH_4^+–N, produced by urea hydrolysis and mineralization, was nitrified into NO_3^-–N or absorbed directly by rice roots; NO_3^-–N, if not denitrified, was easily vertically transported along with soil water flow. These values were consistent with the results (a 9.3 kg ha^{-1} leaching loss with a 250 kg ha^{-1} N application) reported by Zhu et al. (2000) in the same region. Zhao et al. (2012) estimated that the N loads in percolation water at 100 cm in TPR fields were between 3.46 and 5.82 kg ha^{-1} during the 2007–2009 rice seasons in this region.

3.6. Nitrification and denitrification

Paddy soils are dynamic environments, and the transport of N and its transformations in the soil profile are very complex and vary in time depending on alternate wetting and drying conditions (Lüdemann et al., 2000; Ishii et al., 2011). Additionally, the crop roots and microorganisms, variably distributed in the soil, significantly affect the N transformations and thus further complicate N distribution in the soil. Nitrification and denitrification are two important processes in paddy fields, both significantly affected by many soil environmental factors, such as the degree of saturation, oxygen concentrations, and temperature.

Table 4 lists the simulated nitrification and denitrification in each soil layer during the two seasons. No visible differences were found for both nitrification and denitrification among the 2008 and 2009 seasons. However, significant differences existed between different soil layers. Nitrification (on average 90.7%) and denitrification (on average 69.0%) predominantly occurred in the top two soil layers (in the root zone) and decreased quickly in deeper layers. These are significantly affected by the distribution of oxygen in soil. Oxygen concentrations in the soil usually show vertical gradients with soil depth (Lüdemann et al., 2000) and radial gradients with distance from the root surface (Revsbech et al., 1999). A large amount of the surface roots of DSR may be advantageous in obtaining oxygen from floodwater (Naklang et al., 1996). Zhang et al. (2011a,b) also reported that the nitrification decreased and denitrification increased with soil depth (in 0–20 cm) in DSR experimental

fields. When soil is subjected to aerobic–anaerobic cycles, nitrate concentrations tend to increase during aerobic periods but then rapidly decrease when fields are flooded, with soil nitrate presumably lost due to denitrification (Becker et al., 2007; Linquist et al., 2011).

Overall, during the two seasons, the simulated nitrification and denitrification averaged 1.4 and 1.0 kg N ha^{-1} day^{-1}, respectively. Zhou et al. (2012) reported in-situ denitrification, directly determined in the drained-reflooded paddy soil (with TPR), ranging from 0.05 to 10.35 kg N ha^{-1} day^{-1} (averaging 38.9% of applied N), and rates in the continuously flooded paddy soil ranging from 0.05 to 3.18 kg N ha^{-1} day^{-1} (an average of 9.9% of applied N).

3.7. Nitrogen balance

The analysis of the N balance is very important for understanding how efficiently fertilizer is utilized by crops and how much is lost due to various processes. The two dominant inputs of mineral N to paddy fields were from fertilizer applications and mineralization of organic N, which were considered in the model simulations. Other N inputs, such as from dry or wet depositions or from irrigation water, were neglected in the model. As listed in Table 5, simulated outputs of N from a 60 cm soil column mainly include AV (accounting on average for 16.6% of the TNI), crop uptake (31.5%), and denitrification (38.8%). The main difference of N loss between the two seasons was due to surface runoff. The other components of N output were similar. Both AV and denitrification made a significant contribution to the N loss from the DSR field, together accounting for about 55.5% of the TNI. N runoff and leaching were the two main pathways of N pollution from agricultural lands to water systems (Zhao et al., 2012). N leaching at the 60 cm depth and N runoff together accounted for 10.5% of TNI on average. The soil N storage increased by 17.3 kg ha^{-1} on average, with 77% due to NO_3^-–N, which was similar to observed data. The total N balance errors of simulations were less than 1.0% across the two seasons. Overall, simulated N balance components using Hydrus-1D matched corresponding observed data well.

Table 4
Simulated nitrification and denitrification (kg ha^{-1}) in each soil layer in the DSR field during the 2008 and 2009 seasons.

Soil depth (cm)	2008 season		2009 season	
	Nitrification	Denitrification	Nitrification	Denitrification
0–20	120.2	48.2	116.6	47.7
20–40	67.5	57.5	69.7	58.9
40–60	16.3	30.4	16.6	31.4
60–80	1.6	9.9	1.7	10.4
80–100	0.6	3.7	0.6	4.0
100–120	0.5	2.6	0.5	2.9
Total	206.7	152.3	205.7	155.3

Table 5
Components of nitrogen balance (kg ha^{-1}) in a 60-cm soil column of the direct-seeded-rice field during the 2008 and 2009 seasons.

	Riceseason	F	M	AV	D	SR	L	CU	SS	δ
2008	Simulated	220	145.5	−63.4	−136.1	−10.3	−25.3	−114.8	−17.6	−2.0
	Observed			−56.2	–	−9.2	−27.2	−107.3	−11.7	–
2009	Simulated	220	147.8	−58.6	−138.0	−17.0	−24.7	−112.1	−16.9	−0.5
	Observed			−52.6	–	−19.2	−26.2	−104.2	−11.9	–
2009[a]	Simulated	270	142.9	−74.9	−176.2	−18.4	−10.4	−113.0	−17.4	2.6
2009[a]	Simulated	270	117.6	−70.4	−166.2	−16.6	−10.1	−108.0	−13.3	3.0

F–fertilizer, M–mineralization, AV–ammonia volatilization, D–denitrification, SR–surface runoff, L–leaching, CU–crop uptake, SS–change in soil storage, δ–total nitrogen balance error.
[a] Hypothetical scenarios with different fertilizer management discussed in Section 3.8.

3.8. Alternative scenarios

It should be noted that the two evaluated seasons (2008 and 2009) had very different rainfall and irrigation management (Li et al., 2014). Consequently, the upper boundary conditions for water flow substantially differed. However, since applied irrigations more or less balanced rainfalls and corresponding surface runoff, subsurface flow during the two seasons was relatively similar.

On the other hand, fertilizer managements were very similar during the two seasons. To evaluate how the model would respond to different fertilizer managements, we repeated simulations for the 2009 season with the following fertilizer applications (partly based on the study of Li et al. (2010) during the 2007 season): 54, 54, 54, 54, 54, and 71, 71, 0, 67.5, 40.5 kg N ha^{-1} for the base and four top-dressed fertilizer applications, respectively. The total applied N in these two scenarios thus was 270 kg N ha^{-1}, compared to 220 kg N ha^{-1} in our study. For these two scenarios, the model predicted that the N loss due to AV fluxes was 74.9 and 70.4 kg N ha^{-1} (Table 5), respectively, compared to 70.5 and 78.4 kg N ha^{-1} measured during the 2007 season, with slightly different flow (rainfall, irrigation) conditions (Li et al., 2010). These additional two hypothetical scenarios document that different fertilizer managements, as well as climate conditions and water managements, influence the quantity and pathways of nitrogen loss and that the calibrated Hydrus-1D model can be a useful tool in quantifying these different factors in hypothetical or future scenarios.

4. Conclusions

Nitrogen pollution derived from agricultural fields increased the risks of surface water eutrophication and groundwater contamination, especially during the rice season. Cultivation of direct-seeded-rice in many Asian countries induced a different nitrogen fertilizer management in paddy fields compared to fields with traditional transplanted rice, and thus consequently revealed different nitrogen losses into surface water and groundwater environments. The nitrogen balance in a direct-seeded-rice field in the Taihu Lake Basin during two seasons (2008 and 2009) were simulated using Hydrus-1D with prior simulations of water flow and water balance as reported by Li et al. (2014). Simulated nitrogen concentrations at different depths, ammonia volatilization fluxes, and nitrogen leaching fluxes matched the observed values well. This indicates that Hydrus-1D can be a useful tool for simulating the nitrogen transport and transformation processes in a direct-seeded-rice field.

Fertilizer applications and mineralization of organic N were the two most important nitrogen inputs to the paddy field in our study. Ammonia volatilization (on average 16.0% of the total nitrogen input) is a significant nitrogen loss process in DSR fields. The loss of nitrogen due to surface runoff significantly differed between the 2008 (2.8% of TNI) and 2009 (4.6% of TNI) seasons, which had different rainfall/irrigation distributions. The nitrification and denitrification processes occurred mainly in the root zone where a variable, oxidation-reduction environment alternated with drying and wetting conditions. The analysis of the nitrogen balance during the two seasons shows that on average, about 35.5% of total N is removed from the soil profile by rice root uptake, about 2.7% (at 120 cm) leaches to groundwater, and about 22.2% is lost due to denitrification.

References

Allen, R.G., Pereira, L.S., Raes, D., Smith, M., 1998. Crop Evapotranspiration–Guidelines for Computing Crop Water Requirements. FAO, Rome (Irrigation and Drain. Paper No. 56).

Antonopoulos, V.Z., 2010. Modelling of water and nitrogen balances in the ponded water and soil profile of rice fields in Northern Greece. Agric. Water Manag. 98 (2), 321–330.

Becker, M., Asch, F., Maskey, S.L., Pande, K.R., Shah, S.C., Shrestha, S., 2007. Effects of transition season management on soil N dynamics and system N balances in rice–wheat rotations of Nepal. Field Crops Res. 103 (2), 98–108.

Brar, H.S., Bhullar, M.S., 2013. Nutrient uptake by direct seeded rice and associated weeds as influenced by sowing date, variety and weed control. Indian J. Agric. Res. 47 (4), 353–358.

Cao, Y., Tian, Y., Yin, B., Zhu, Z., 2013. Assessment of ammonia volatilization from paddy fields under crop management practices aimed to increase grain yield and N efficiency. Field Crops Res. 147, 23–31.

Chandna, P., Khurana, M.L., Ladha, J.K., Punia, M., Mehla, R.S., Gupta, R., 2011. Spatial and seasonal distribution of nitrate-N in groundwater beneath the rice–wheat cropping system of India: A geospatial analysis. Environ. Monit. Assess. 178, 545–562.

Chen, C.F., Chiang, P.S., 1963. Ammonium ion adsorption of some paddy soils. Acta Pedol. Sin. 11 (2), 171–184.

Chen, S., Cai, S.G., Chen, X., Zhang, G.P., 2009. Genotypic differences in growth and physiological responses to transplanting and direct seeding cultivation in rice. Rice Sci. 16 (2), 143–150.

Chowdary, V.M., Rao, N.H., Sarma, P.B.S., 2004. A coupled soil water and nitrogen balance model for flooded rice fields in India. Agric. Ecosyst. Environ. 103 (3), 425–441.

Duan, Y., Yin, X., Zhang, Y., Shen, Q., 2007. Mechanisms of enhanced rice growth and nitrogen uptake by nitrate. Pedosphere 17 (6), 697–705.

Farooq, M., Siddique, K.H.M., Rehman, H., Aziz, T., Lee, D., Wahid, A., 2011. Rice direct seeding: experiences, challenges and opportunities. Soil Tillage Res. 111 (2), 87–98.

Feddes, R.A., Kowalik, P.J., Zaradny, H., 1978. Simulation of Field Water Use and Crop Yield. John Wiley & Sons, New York (Online).

Hanson, B.R., Šimůnek, J., Hopmans, J.W., 2006. Evaluation of urea–ammonium–nitrate fertigation with drip irrigation using numerical modeling. Agric. Water Manag. 86 (1–2), 102–113.

Hayashi, S., Kamoshita, A., Yamagishi, J., Kotchasatit, A., Jongdee, B., 2007. Genotypic differences in grain yield of transplanted and direct-seeded rainfed lowland rice (Oryza sativa L.) in northeastern Thailand. Field Crops Res. 102, 9–21.

Hou, H., Zhou, S., Hosomi, M., Toyota, K., Yosimura, K., Mutou, Y., Nisimura, T., Takayanagi, M., Motobayashi, T., 2007. Ammonia emissions from anaerobically digested slurry and chemical fertilizer applied to flooded forage rice. Water Air Soil Pollut. 183 (1–4), 37–48.

Ishii, S., Ikeda, S., Minamisawa, K., Senoo, K., 2011. Nitrogen cycling in rice paddy environments: past achievements and future challenges. Microbes Environ. 26 (4), 282–292.

Jeon, J., Yoon, C.G., Ham, J., Jung, K., 2004. Model development for nutrient loading estimates from paddy rice fields in Korea. J. Environ. Sci. Health Part B Pestic. Food Contam. Agric. Wastes B39 (5–6), 845–860.

Jury, W.A., Spencer, W.F., Farmer, W.J., 1983. Behavior assessment model for trace organics in soil I. Model description. J. Environ. Qual. 12 (4), 558–564.

Kirk, G.J.D., Solivas, J.L., Begg, C.B.M., 1994. The rice root–soil interface. In: Kirk, G.J.D. (Ed.), Rice Roots: Nutrient and Water Use. International Rice Research Institute, Los Banos, Philippines, pp. 1–10.

Kirk, G.J.D., Kronzucker, H.J., 2005. The potential for nitrification and nitrate uptake in the rhizosphere of wetland plants: a modeling study. Ann. Bot. 96, 639–646.

Kumar, V., Ladha, J.K., 2011. Direct seeding of rice: recent developments and future research needs. In: Donald, L.S. (Ed.), Advances in Agronomy. Academic Press, pp. 297–413.

Kyaw, K.M., Toyota, K., Okazaki, M., Motobayashi, T., Tanaka, H., 2005. Nitrogen balance in a paddy field planted with whole crop rice (Oryza Sativa Cv. Kusahonami) during two rice-growing seasons. Biol. Fertil. Soils 42 (1), 72–82.

Li, B., Xin, W., Sun, S., Shen, Q., Xu, G., 2006. Physiological and molecular responses of nitrogen-starved rice plants to re-supply of different nitrogen sources. Plant Soil 287, 145–159.

Li, H., Liang, X., Chen, Y., Tian, G., Zhang, Z., 2008. Ammonia volatilization from urea in rice fields with zero-drainage water management. Agric. Water Manag. 95 (8), 887–894.

Li, W.J., Xia, Y.Q., Ti, C.P., Yan, X.Y., 2011. Evaluation of biological and chemical nitrogen indices for predicting nitrogen-supplying capacity of paddy soils in the Taihu Lake region, China. Biol. Fertil. Soils 47, 669–678.

Li, Y., Šimůnek, J., Jing, L.F., Zhang, Z.T., Ni, L.X., 2014. Evaluation of water movement and water losses in a direct-seeded-rice field experiment using Hydrus-1D. Agric. Water Manag. 142, 38–46.

Li, Y., Yang, L.Z., Wang, C., 2010. Evaluation of fertilizing schemes for direct-seeding rice fields in Taihu Lake Basin, China. Turk. J. Agric. For. 34, 83–90.

Li, Y., Wang, X., 2013. Root-induced changes in radial oxygen loss, rhizosphere oxygen profile, and nitrification of two rice cultivars in Chinese red soil regions. Plant Soil 365 (1–2), 115–126.

Linquist, B.A., Koffler, K., Hill, J.E., van Kessel, C., 2011. Rice field drainage affects nitrogen dynamics and management. Calif. Agric. 65 (2), 80–84.

Lüdemann, H., Arth, I., Liesack, W., 2000. Spatial changes in the bacterial community structure along a vertical oxygen gradient in flooded paddy soil cores. Appl. Environ. Microbiol. 66 (2), 754–762.

Mnguu, Y.O., 2010. Effect of crop management practices on Nitrogen (N) availability and N use efficiency in direct wet seeded rice. J. Anim. Plant Sci. 6 (1), 589–596.

Najafi, N., 2013. Changes in pH, EC and concentration of phosphorus in soil solution during submegence and rice growth period in some paddy soils of north of Iran. Int. J. Agric. Res. Rev. 3 (2), 271–280.

Nakasone, H., Abbas, M.A., Kuroda, H., 2004. Nitrogen transport and transformation in packed soil columns from paddy fields. Paddy Water Environ. 2 (3), 115–124.

Naklang, K., Fukai, S., Nathabut, K., 1996. Growth of rice cultivars by direct seeding and transplanting under upland and lowland conditions. Field Crops Res. 48 (2–3), 115–123.

Phogat, V., Mahadevan, M., Skewes, M., Cox, J.W., 2012. Modelling soil water and salt dynamics under pulsed and continuous surface drip irrigation of almond and implications of system design. Irrig. Sci. 30 (4), 315–333.

Phogat, V., Yadav, A.K., Malik, R.S., Kumar, S., Cox, J., 2010. Simulation of salt and water movement and estimation of water productivity of rice crop irrigated with saline water. Paddy Water Environ. 8 (4), 333–346.

Qiao, J., Yang, L., Yan, T., Xue, F., Zhao, D., 2012. Nitrogen fertilizer reduction in rice production for two consecutive years in the Taihu Lake area. Agric. Ecosyst. Environ. 146 (1), 103–112.

Ramos, T.B., Šimůnek, J., Gonçalves, M.C., Martins, J.C., Prazeres, A., Pereira, L.S., 2012. Two-dimensional modeling of water and nitrogen fate from sweet sorghum

irrigated with fresh and blended saline waters. Agric. Water Manag. 111, 87–104.

Ravikumar, V., Vijayakumar, G., Šimůnek, J., Chellamuthu, S., Santhi, R., Appavu, K., 2011. Evaluation of fertigation scheduling for sugarcane using a vadose zone flow and transport model. Agric. Water Manag. 98 (9), 1431–1440.

Renard, J.J., Calidonna, S.E., Henley, M.V., 2004. Fate of ammonia in the atmosphere—a review for applicability to hazardous releases. J. Hazard. Mater. 108 (1–2), 29–60.

Revsbech, N.P., Pedersen, O., Reichardt, W., Briones, A., 1999. Microsensor analysis of oxygen and pH in the rice rhizosphere under field and laboratory conditions. Biol. Fertil. Soils 29 (4), 379–385.

Rice, C.W., Smith, M.S., 1984. Short-term immobilization of fertilizer nitrogen at the surface of no-till and plowed soils. Soil Sci. Soc. Am. J. 48 (2), 295–297.

Roberts, T.L., Ross, W.J., Norman, R.J., Slaton, N.A., Wilson, C.E., 2011. Predicting nitrogen fertilizer needs for rice in Arkansas using alkaline Hydrolyzable-Nitrogen. Soil Sci. Soc. Am. J. 75 (3), 1–11.

Sarkar, M.C., Banerjee, N.K., Rana, D.S., Uppal, K.S., 1991. Field measurements of ammonia volatilization losses of nitrogen from urea applied to wheat. Fertil. News 36, 25–28.

Sasakawa, H., Yamamoto, Y., 1978. Comparison of the uptake of nitrate and ammonium by rice seedlings. Plant Physiol. 62, 665–669.

Schnier, H.F., Dingkuhn, M., Datta, S.K.D., Marqueses, E.P., Faronilo, J.E., 1990. Nitrogen-15 balance in transplanted and direct-seeded flooded rice as affected by different methods of urea application. Biol. Fertil. Soils 10 (2), 89–96.

Šimůnek, J., van Genuchten, M.T., Šejna, M., 2008. Development and applications of the HYDRUS and STANMOD software packages, and related codes. Vadose Zone J. 7 (2), 587–600.

Šimůnek, J., Hopmans, J.W., 2009. Modeling compensated root water and nutrient uptake. Ecol. Model. 220 (4), 505–521.

Singh, U., Sanabria, J., Austin, E.R., Agyin-Birikorang, S., 2011. Nitrogen transformation, ammonia volatilization loss, and nitrate leaching in organically enhanced nitrogen fertilizers relative to urea. Soil Sci. Soc. Am. J. 76, 1842–1854.

Sutanto, S.J., Wenninger, J., Coenders-Gerrits, A.M.J., Uhlenbrook, S., 2012. Partitioning of evaporation into transpiration, soil evaporation and interception: a comparison between isotope measurements and a HYDRUS-1D model. Hydrol. Earth Syst. Sci. 16 (8), 2605–2616.

Wang, M.Y., Class, A.D.M., Shaff, J.E., Kochian, L.V., 1994. Ammonium uptake by rice roots: III. Electrophysiology. Plant Physiol. 104 (3), 899–906.

Weerakoon, W.M.W., Mutunayake, M.M.P., Bandara, C., Rao, A.N., Bhandari, D.C., Ladha, J.K., 2011. Direct-seeded rice culture in Sri Lanka: lessons from farmers. Field Crops Res. 121 (1), 53–63.

Yadav, S., Gill, M.S., Kukal, S.S., 2007. Performance of direct-seeded basmati rice in loamy sand in semi-arid sub-tropical India. Soil Tillage Res. 97 (2), 229–238.

Yan, D., Wang, D., Sun, R., Lin, J., 2006. N mineralization as affected by long-term N fertilization and its relationship with crop N uptake. Pedosphere 16 (1), 125–130.

Yin, X.Y., Xu, Y.C., Shen, Q.R., Zhou, C.L., Dittert, K., 2004. Absorption and apparent budget of nitrogen by direct-seeding rice cultivated in aerobic soil with or without mulching. Acta Ecol. Sin. 24 (8), 1575–1581.

Zhang, C., Xu, Y., Zhao, H., Tu, E., Shen, Q., Zhang, Y., 2011a. Effects of different nitrogen forms on nitrogen uptake and root growth of rice at the seedling stage. J. Nanjing Agric. Univ. 34 (3), 72–76.

Zhang, J.S., Zhang, F.P., Yang, J.H., Wang, J.P., Cai, M.L., Li, C.F., Cao, C.G., 2011b. Emissions of N_2O and NH_3, and nitrogen leaching from direct seeded rice under different tillage practices in central China. Agric. Ecosyst. Environ. 140 (1–2), 164–173.

Zhang, Q., Wang, G., 2002. Optimal nitrogen application for direct-seeding early rice. Chin. J. Rice Sci. 16 (4), 346–350.

Zhao, X., Zhou, Y., Min, J., Wang, S., Shi, W., Xing, G., 2012. Nitrogen runoff dominates water nitrogen pollution from rice–wheat rotation in the Taihu Lake region of China. Agric. Ecosyst. Environ. 156, 1–11.

Zhou, S., Sakiyama, Y., Riya, S., Song, X., Terada, A., Hosomi, M., 2012. Assessing nitrification and denitrification in a paddy soil with different water dynamics and applied liquid cattle waste using the 15N isotopic technique. Sci. Total Environ. 430, 93–100.

Zhu, J.G., Han, Y., Liu, G., Zhang, Y.L., Shao, X.H., 2000. Nitrogen in percolation water in paddy fields with a rice/wheat rotation. Nutr. Cycl. Agroecosyst. 57 (1), 75–82.

Zhu, Z.L., Fan, X.H., Sun, Y.H., Wang, D.J., 2004. Nitrogen-cycle in an early-rice field and its environmental effects in Taihu Lake Region. Crop Res. 4, 187–191 (In Chinese with English Abstract).